THE ASTROPHYSICAL JOURNAL, 459:73–81, 1996 March 1

3C 279 MULTIWAVELENGTH MONITORING. II. THE GROUND-BASED CAMPAIGN

P. GRANDI,[1,2] C. M. URRY,[1] L. MARASCHI,[3] A. E. WEHRLE,[4] G. M. MADEJSKI,[5] M. F. ALLER,[6] H. D. ALLER,[6] C. D. BAILYN,[7] T. J. BALONEK,[8] T. H. BOCK,[9] I. S. GLASS,[10] S. J. LITCHFIELD,[11,12] I. M. MCHARDY,[13] J. S. MULCHAEY,[2,14] H.-P. REUTER,[15] E. I. ROBSON,[11,16] A. C. SADUN,[17] W. SHERRY,[7] H. STEPPE,[15] J. A. STEVENS,[11] H. TERÄSRANTA,[18] M. TORNIKOSKI,[18] AND S. J. WAGNER[9]

Received 1995 March 15; accepted 1995 July 11

ABSTRACT

The optically violently variable quasar 3C 279 was monitored simultaneously from radio to γ-ray frequencies in 1992 December–1993 January. We report a detailed study of the ground-based results from radio to optical wavelengths. These data show that 3C 279 has a typical blazar spectrum, slightly rising at radio frequency and then progressively steeper above a first turnover frequency between 37 and 90 GHz. In the millimeter wavelength region, a simple power law is not an adequate description of the spectrum. We suggest that the millimeter "shoulder" corresponds to an additional emission component, self-absorbed between 150 and 375 GHz, possibly associated with the detachment of a new VLBI knot and with the start of radio flare.

A flux increase of 20% over 20 days was observed at 37 and 90 GHz, while contemporaneously the *R*-band flux doubled in about two weeks. The lack of strong variability in contemporaneous X-ray light curves (possible X-ray variations are less than 30%) implies no direct (i.e., zero lag) correlation between the optical and X-ray fluxes. If X-rays are produced by inverse-Compton scattering of relativistic electrons on some seed photons, the above results exclude that the observed optical photons are the seeds and/or that the relativistic electrons radiating via synchrotron in the optical band are responsible for the scattering to X-ray energies. We suggest that the X-rays are instead produced through the inverse-Compton process by electrons of lower energy, which radiate via synchrotron in the radio to millimeter wave bands and which scatter either on the synchrotron photons themselves or on external photons.

Subject headings: galaxies: photometry — gamma rays: observations — quasars: individual (3C 279) — radiation mechanisms: nonthermal — X-rays: galaxies

1. INTRODUCTION

The source 3C 279 is a well-known optically violent variable (OVV) quasar. It was the first source found to show superluminal motion (Whitney et al. 1971; Cotton et al. 1979; Unwin et al. 1989) and the first blazar detected in gamma rays with the *Compton Gamma Ray Observatory* (*CGRO*; Hartman et al. 1992). The quasar 3C 279 is characterized by intense flux variability from radio to gamma-ray frequencies on timescales of weeks and months (Pica et al. 1980; Mead et al. 1990; Webb et al. 1990; Hughes, Aller, & Aller 1991; Makino et al. 1989, 1992; Takalo et al. 1992; Teräsranta et al. 1992; Kniffen et al. 1993; Bonnell, Vestrand, & Stacy 1994; Grandi et al. 1994; Shrader et al. 1994; Stevens et al. 1994; Litchfield et al. 1995). In the optical range, brightness variations of more than a magnitude in only 1 day have been observed (Webb et al. 1990; Sadun, Fajardo, & Carini 1992). In the X-ray band, rapid large-amplitude variability seems uncommon, though a variation of $\sim$20% was detected on a timescale of hours (Makino et al. 1989, 1992). In the gamma-ray band, the flux was observed to vary by a factor of 2 in few days (Kniffen et al. 1993).

The quasar 3C 279 has a typical blazar spectrum. The very high percentage of polarized flux suggests the radio through optical emission is dominated by synchrotron radiation (Aller, Hughes, & Aller 1991; Mead et al. 1990). When plotted as power per logarithmic bandwidth (νF_ν vs. ν), the energy distribution of 3C 279 increases from radio to millimeter wavelengths and then decreases in the infrared-optical-UV region (Landau et al. 1985; Brown et al. 1989;

[1] Space Telescope Science Institute, 3700 San Martin Drive, Baltimore, MD 21218.
[2] Present address: Istituto di Astrofisica Spaziale - CNR, Via E. Fermi 21, I-00044 Frascati (Roma), Italy.
[3] Department of Physics, University of Milan, Via Celoria 16, I-20133 Milan, Italy.
[4] Caltech 100-22, Infrared Processing Analysis Center, 770 S. Wilson, Pasadena, CA 91125.
[5] NASA/Goddard Space Flight Center, Code 666, Greenbelt, MD 20771.
[6] University of Michigan, Physics and Astronomy, 817 Dennison Building, Ann Arbor, MI 48109.
[7] Yale University, Department of Astronomy, Box 208101, New Haven, CT 06520-8101.
[8] Department of Astronomy, Colgate University, 13 Oak Drive, Hamilton, New York 13346.
[9] Landessternwarte Heidelberg-Konigstühl, Konigstühl, D-6900 Heidelberg, Germany.
[10] South African Astronomical Observatory, P.O. Box 9, Observatory 7935.
[11] Centre for Astrophysics, University of Central Lancashire, Preston, PR1 2HE, UK.
[12] Present address: University of Crete, Department of Physics, 714 09 Heraklion, Crete, Greece.
[13] Department of Physics, University of Southampton, Southampton SO9 5NH, UK.
[14] Present address: The observatories of the Carnegi Institution of Washington, 813 Santa Barbara Street, Pasadena, CA 91101.
[15] Istituto De Radioastronomia Millimetrica, Avenida Divina Pastora 7, Nucleo Central, E-18012 Granada, Spain.
[16] Joint Astronomy Centre, 660 N. Aohoku Place, University Park, Hilo, HI 96720.
[17] Bradley Observatory, Agnes Scott College, Decatur, GA 30030.
[18] Metsahovi Radio Research Station, 02540 Kylmala, Finland.

Makino et al. 1989; Maraschi et al. 1994). The location of the peak power output is uncertain owing to the general lack of data between the millimeter and IR spectral domains. The energy distribution rises again from X-rays to gamma rays, where the apparent emitted power can greatly exceed that in all other bands combined, when the source is in outburst (Hartman et al. 1992).

The unexpected discovery of such strong gamma-ray emission from 3C 279 as well as from many other blazars (Hartman et al. 1994; von Montigny et al. 1995) has refocused attention on theoretical models. While our understanding of the emission processes at low energies is fairly good, the situation at higher energies is less clear. X-ray and gamma-ray photons can be produced through Comptonization of radio, optical, and UV radiation by relativistic electrons in a jet, but the origin of the soft photons is uncertain. They could be synchrotron photons (the synchrotron self-Compton, or SSC, mechanism; Maraschi, Ghisellini & Celotti 1992, Bloom & Marscher 1993), or photons produced external to the jet, such as UV and X-ray radiation from an accretion disk (Dermer, Schlickeiser, & Mastichiadis 1992; Zbyszewska 1993), or reprocessed radiation from emission-line clouds and intercloud gas (Blandford 1993; Sikora, Begelman, & Rees 1994; Blandford & Levinson 1995). These models, which can reproduce the spectra of blazars reasonably well, predict strong but different correlations among the wave bands.

Multiwavelength studies are essential to discriminate among possible theoretical interpretations, through the detection of spectral variability and correlations among different wave bands. In an effort to understand the physical mechanisms in blazars, a multifrequency campaign to observe 3C 279 was organized for an $\sim$1 month period in 1992 December–1993 January. Data were obtained at radio through gamma-ray frequencies, with particularly good temporal coverage with the *ROSAT*, *IUE*, and *CGRO* satellites, showing that 3C 279 was in a low state throughout the campaign. The average low-state spectrum and a comparison to the brighter state observed in 1991 can be found in Maraschi et al. (1994).

Here we present the full results from ground-based monitoring observations obtained during the campaign; the UV and X-ray observations will be discussed by Urry et al. (1995). VLBI observations of 3C 279 at 22 and 5 GHz were also made about 1 month before and after the campaign. These images resolved the jet within a few hundred parsecs of the nucleus. A detailed discussion of the VLBI results will be reported by Wehrle et al. (1995). The structure of this paper is as follows: the relevant information about the data is given in § 2; the multifrequency light curves and radio-through-optical spectra are presented in § 3, and the implications for theoretical models are discussed in § 4.

2. OBSERVATIONS

The quasar 3C 279 was monitored from the ground from radio through optical frequencies in 1992 December–1993 January, simultaneously with the 21 day pointing at the source by *CGRO* (from 1992 December 22 through 1993 January 12). The bulk of the multifrequency observations covered the same period, with additional data collected immediately before and after.

During the campaign, 3C 279 was at a relatively low luminosity level. In early 1992 December, just prior to the observing campaign, the *R* magnitude was estimated by T. Balonek to be 17.3 mag, the faintest in about 6 years. The *ROSAT* satellite observed a 1 keV flux lower by a factor $\sim$8 than that measured by *Ginga* in 1988 July (Makino et al. 1989; Maraschi et al. 1994). Due to the faintness of the source, only an average flux value for the whole 20 day pointing could be derived from the *CGRO* data, and this flux was $\sim$40 times lower than the peak of the 1991 June flare (Kniffen et al. 1993; Maraschi et al. 1994). In spite of this, considerable data were collected during the multifrequency monitoring. All the measurements between 1992 December 1 and 1993 January 31 are summarized in Table 1, which lists who contributed the particular data (col. [1]), the data of the observations in year-month-day (col. [2]) and Julian day (col. [3]), the frequency of observation in logarithmic units (col. [4]), the flux in Janskys (col. [5]), and the 1 σ error (col. [6]).

We group the observations in three wavelength intervals: radio observations (4.8–37 GHz) in § 2.1, millimeter observations (90 GHz–0.8 mm) in § 2.2, and infrared-optical observations (2.2–0.44 μm) in § 2.3.

2.1. *Radio Observations*

Radio flux densities were obtained at 4.8, 8, and 14.5 GHz by H. Aller and M. Aller using the Michigan Radio Telescope. The sparse temporal sampling was the result of a combination of technical problems and bad weather during 1993 January. At 22 and 37 GHz, almost daily observations were performed with the Metsähovi Radio Research Station (in Finland) throughout the whole campaign. Details about the reduction of these two data sets can be found in Hughes et al. (1991) and Teräsranta et al. (1992), respectively. The derived flux densities are reported in Table 1.

2.2. *Millimeter Observations*

Millimeter data were collected at 90 GHz (3.3 mm) and 230 GHz (1.3 mm) by H. Steppe and H.-P. Reuter with the 30 cm telescope of the Instituto de Radioastronomia Millimetrica (IRAM). Details on data reduction can be found in Steppe et al. (1988, 1992). The data cover a period of about a month from December 17 to January 15, albeit with sparse sampling. Additional data at 90 GHz were obtained by T. Balonek at the National Radio Astronomy Observatory (NRAO)[19] during the first two weeks of December. One observation at 90 GHz was also obtained by M. Tornikoski at the SEST (La Silla) on 1992 December 31 (see Tornikoski et al. 1995 for reduction procedure).

Data were also obtained at 375 GHz (0.8 mm), 270 GHz (1.1 mm), and 150 GHz (2.0 mm) by I. McHardy and collaborators. These data were taken with the ^{3}He-cooled facility bolometer, UKT14 (Duncan et al. 1990), at the 15 m James Clerk Maxwell Telescope (JCMT). Calibration was made primarily with respect to the JCMT standard source 16293 – 2422 (Sandell 1994), and the atmospheric extinction was corrected for in the manner described by Stevens & Robson (1994).

2.3. *Infrared-Optical Observations*

Infrared *JHK* photometry was obtained by I. Glass at the 1.9 m telescope at Sutherland (South Africa) with the MKIII infrared photometer on 1993 January 12, a few days

[19] The NRAO is operated by Associated Universities Inc., under cooperative agreement with the National Science Foundation.

TABLE 1

3C 279 MULTIFREQUENCY DATA

Observers	Date[a]	JDay	log ν[b]	Flux (Jy)	σ_F (Jy)
Aller & Aller	921212	2448969.1	9.68 (4.8 GHz)	10.59	0.12
Univ. Michigan	930103	2448991.0		10.42	0.27
	930123	2449010.9		10.56	0.12
	921225	2448982.1	9.90 (8.0 Ghz)	12.36	0.24
	921226	2448983.0		12.53	0.11
	930101	2448989.0		12.23	0.25
	930107	2448995.0		12.27	0.09
	930120	2449009.0		12.41	0.12
	921201	2448958.2	10.16 (14.5 GHz)	13.56	0.12
	921202	2448959.1		13.66	0.31
	921207	2448964.1		13.72	0.12
	921208	2448965.1		13.88	0.19
	921219	2448976.0		14.04	0.10
	921220	2448977.0		13.72	0.19
	921223	2448980.0		13.63	0.27
	921229	2448986.0		13.24	0.20
	921230	2448987.0		12.48	0.37
	930101	2448989.0		13.87	0.12
	930127	2449014.9		13.07	0.15
Teräsranta	921210	2448966.7	10.34 (22 GHz)	15.61	0.44
Metsahovi Radio Stat.	921212	2448968.8		15.88	0.47
	921218	2448974.7		15.73	0.46
	921220	2448976.7		15.60	0.51
	921221	2448977.7		14.25	0.41
	921222	2448978.7		15.50	0.46
	921223	2448979.7		15.15	0.44
	921224	2448980.7		15.41	0.45
	921226	2448982.7		15.23	0.45
	921227	2448983.7		15.66	0.53
	921228	2448984.7		14.73	0.43
	921229	2448985.7		15.71	0.44
	921230	2448986.7		15.45	0.44
	921231	2448987.7		15.15	0.42
	930102	2448989.7		14.69	0.47
	930103	2448990.7		14.84	0.51
	930104	2448991.7		16.31	0.47
	930105	2448992.7		14.93	0.43
	930108	2448995.7		15.86	0.46
	930109	2448996.7		16.33	0.49
	921220	2448976.8	10.57 (37 GHz)	16.00	0.56
	921221	2448977.7		16.93	0.50
	921222	2448978.7		16.68	0.47
	921223	2448979.7		16.43	0.46
	921224	2448980.7		16.85	0.45
	921227	2448983.7		16.21	0.53
	921228	2448984.7		16.20	0.45
	921229	2448985.7		16.56	0.47
	921230	2448986.7		16.98	0.45
	921231	2448987.7		16.97	0.45
	930104	2448991.7		17.48	0.47
	930105	2448992.7		17.19	0.47
	930109	2448996.6		19.09	0.52
Balonek	921201	2448958.3	10.95 (90 GHz)	13.65	0.80
NRAO	921210	2448967.3		13.97	0.80
	921213	2448970.3		14.30	0.80
	921217	2448973.8		15.22	0.97
Steppe & Reuter	921217	2448973.8		15.22	0.97
IRAM Granada/Spain	921223	2448979.8		14.79	0.85
	921229	2448985.8		17.20	0.86
	921230	2448986.8		15.64	0.81
	921231	2448987.8		14.96	0.75

TABLE 1—*Continued*

Observers	Date[a]	JDay	log ν[b]	Flux (Jy)	σ_F (Jy)
	930101	2448988.8		14.30	0.79
	930103	2448990.8		15.23	0.76
	930104	2448991.8		15.58	0.78
	930106	2448993.8		16.89	0.85
	930107	2448994.8		17.16	0.86
	930108	2448995.8		15.64	0.79
	930115	2449002.8		16.15	0.84
Tornikoski - Metsahovi Radio Stat.	921231	2448988.6		13.86	0.11
McHardy, Stevens, Litchfield, Robson	921229	2448986.3	11.18 (2.0 mm)	8.60	0.90
JCMT	930114	2449002.3		8.40	0.40
	930115	2449003.3		8.90	0.60
	930119	2449007.3		9.90	0.80
	930120	2449008.3		8.70	0.40
	930121	2449009.3		9.40	0.90
Steppe & Reuter	921223	2448979.8	11.36 (230 GHz)	7.26	1.16
IRAM Granada/Spain	921230	2448986.8		7.02	0.72
	921231	2448987.8		6.94	0.70
	930103	2448990.8		6.90	0.70
	930104	2448991.8		6.83	0.68
	930106	2448992.8		6.76	0.70
	930107	2448994.8		6.90	0.71
McHardy, Stevens, Litchfield, Robson	931230	2448987.3	11.43 (1.1 mm)	7.70	1.20
JCMT	930114	2449002.3		7.80	0.40
	930115	2449003.3		7.70	0.40
	930118	2449006.3		7.50	0.80
	930119	2449007.3		7.60	0.40
	930120	2449008.3		6.60	0.40
	930121	2449009.3		7.00	0.70
	930114	2449002.3	11.57 (0.8 mm)	5.20	0.30
	930115	2449003.3		5.60	0.30
	930118	2449006.3		6.10	0.60
	930119	2449007.3		5.50	0.30
	900120	2449008.3		5.90	0.30
Glass	930112	2448999.6	14.15 (K)	7.98×10^{-3}	0.22×10^{-3}
South African Astron. Obs.	930112	2448999.6	14.25 (H)	4.72×10^{-3}	0.17×10^{-3}
	930112	2448999.6	14.40 (J)	2.61×10^{-3}	0.22×10^{-3}
Bailyn - CTIO	930103	2448990.8	14.58 (I)	1.35×10^{-3}	0.49×10^{-4}
	930104	2448991.8		1.49×10^{-3}	0.54×10^{-4}
	930105	2448992.8		1.68×10^{-3}	0.61×10^{-4}
	930106	2448993.8		1.81×10^{-3}	0.82×10^{-4}
	930103	2448990.8	14.67 (R)	9.05×10^{-4}	0.33×10^{-4}
	930104	2448991.8		1.00×10^{-3}	0.36×10^{-4}
	930105	2448992.8		1.12×10^{-3}	0.40×10^{-4}
	930106	2448993.8		1.17×10^{-3}	0.54×10^{-4}
Wagner & Boch	921228	2448984.6		5.99×10^{-4}	0.27×10^{-4}
Calar Alto	921229	2448985.7		6.86×10^{-4}	0.22×10^{-4}
	921230	2448986.7		7.30×10^{-4}	0.33×10^{-4}
	921231	2448987.6		7.78×10^{-4}	0.25×10^{-4}
	930101	2448988.6		8.37×10^{-4}	0.27×10^{-4}
	930103	2448990.7		1.01×10^{-3}	0.37×10^{-4}
	930104	2448991.7		1.04×10^{-3}	0.47×10^{-4}
	930105	2448992.7		1.08×10^{-3}	0.35×10^{-4}
	930106	2448993.6		1.21×10^{-3}	0.39×10^{-4}
Mulchaey - KPNO	931223	2448980.1	14.67 (R[c])	3.91×10^{-4}	0.84×10^{-4}
Bailyn - CTIO	930103	2448990.8	14.74 (V)	6.62×10^{-4}	0.24×10^{-4}
	930104	2448991.8		7.20×10^{-4}	0.26×10^{-4}
	930105	2448992.8		8.04×10^{-4}	0.29×10^{-4}
	930106	2448993.8		8.49×10^{-4}	0.38×10^{-4}
	930103	2448990.8	14.83 (B)	4.24×10^{-4}	0.15×10^{-4}
	930104	2448991.8		4.91×10^{-4}	0.18×10^{-4}
	930105	2448992.8		5.53×10^{-4}	0.20×10^{-4}
	930106	2448993.8		5.38×10^{-4}	0.29×10^{-4}

[a] Date in year-month-day.
[b] For clarity, we also report in brackets the value of ν, λ, or the filter name.
[c] Harris *R* band.

after the *IUE* and *ROSAT* intensive monitoring period. The comparison star HR 4689 (Carter 1990) was used to compute the 3C 279 fluxes.

Four nights of *BVRI* photometry of 3C 279 were obtained by C. Bailyn and collaborators with the CTIO 0.9 m telescope at Cerro Tololo. Observations in all four bands were repeated several times each night in order to detect fast variability. Additional *R*-band photometry, with excellent time sampling, was obtained daily by S. Wagner using the Calar Alto telescope from 1992 December 28 through 1993 January 6 (except for January 2). When possible, 3C 279 was observed twice per night from Calar Alto. One optical observation in the R Harris band was also made by J. Mulchaey with the 2.1 m telescope at Kitt Peak on 1993 December 23. All the optical observers referenced their 3C 279 magnitudes to six well-calibrated stars found in the 3C 279 field (P. Smith, private communication). The zero magnitude flux density scale was taken from Bessel (1979).

No intranight variability was detected in any optical band. The flux densities given in Table 1 represent average values for each night.

3. RESULTS

3.1. *Multifrequency Light Curves*

The light curves at different frequencies are shown together in Figure 1. A standard χ^2 statistic was used to test time variability, with a threshold for statistical significance at a probability for constant flux less than 10^{-3}.

At 4.8 and 8 GHz, the flux was stable ($\Delta F/F < 3\%$), while at 14.5 GHz some low-level fluctuations were observed ($\Delta F/F \sim 10\%$). While at 22 GHz no significant variability was detected, the 37 GHz flux varied significantly, showing an increasing trend of 20% over 16 days. Day-to-day fluctuations present in both the 22 and 37 GHz data are not statistically significant. Note that the errors at 22 and 37 GHz are sufficiently small that a 20% increase could have been (but is not) detected in the 22 GHz light curve. As discussed in the next session, 37 GHz corresponds to the peak in the spectral flux distribution, that is, to the transition between optically thick and thin radiation.

Combining data from different observatories, NRAO and IRAM, a flux increase of about 20% at 90 GHz seems to be present over the course of the month. No statistically significant variability was detected in the other millimeter data (150–375 GHz). Note, however, that the errors are relatively large and the coverage rather sparse. Variability with the same amplitude and timescale as at 37 and 90 GHz could be present without being detectable in the present data.

The *BVRI* light curves are characterized by a pronounced and fast flux variation. During the first half of January the optical luminosity of 3C 279 increased steadily; in the *R* band, where the sampling is best, the flux doubled in 10 days (from 1992 December 28 to 1993 January 6).

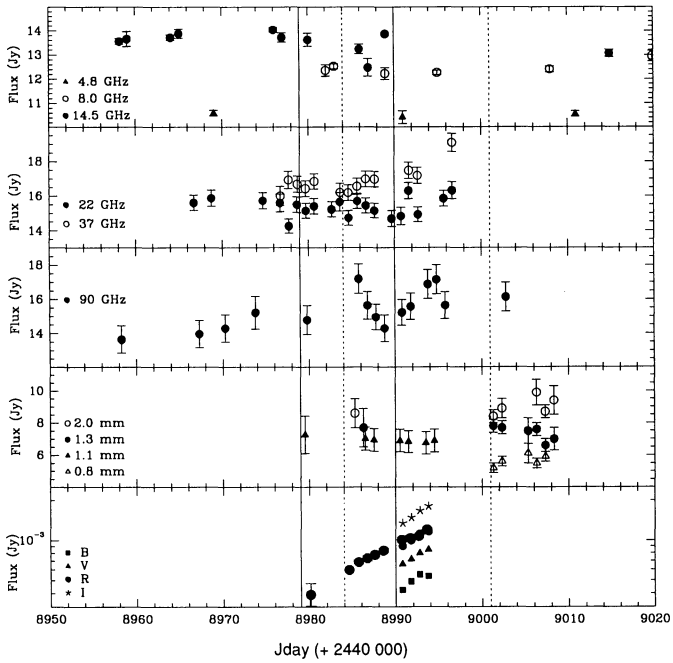

FIG. 1.—Radio, millimeter, and optical light curves collected during the multifrequency campaign from 1992 December 1 to 1993 January 31. Solid vertical lines delimit the time interval of the *CGRO* observation, and dashed lines delimit the time interval of the *ROSAT* observation. Note the rapid doubling of *R*-band flux in 10 days and the smaller but similar trend at 37 GHz.

3.2. *Radio-to-Optical Spectra*

Looking at Figure 1, it is clear that the epoch with best frequency coverage is between 1993 January 3–6. During those days, we have measurements in four optical filters and measurements at 22, 37, and 90 GHz and 1.1 mm. The average values obtained during those three days are shown in Figure 2 as filled circles.

At lower radio frequencies, no variability was observed during the whole campaign; therefore we take the values measured between 1993 January 1–3 (filled circles in Fig. 2). The only measurement in the infrared (*J*, *H*, and *K*) is on January 12, and on January 14 measurements at more millimeter frequencies are available. As a result of the strong increasing trend observed in the optical in the preceding days, the nonsimultaneity of the latter may introduce an unknown shift, so the latter points are shown in Figure 2 with open symbols.

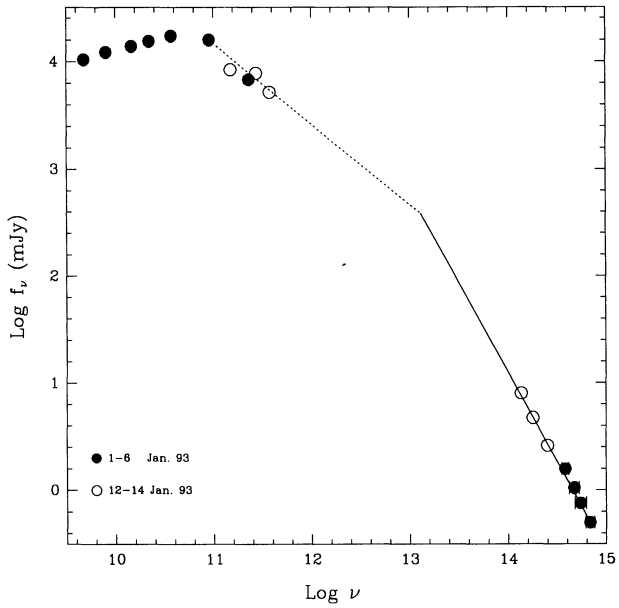

FIG. 2.—The radio-through-optical spectrum of 3C 279 during our campaign. The extrapolation of the millimeter (*dashed line*) and infrared-optical (*solid line*) power-law fits suggests the presence of a break frequency above 10^{13} Hz.

Typical blazar spectra over the radio through optical range can be described by a series of power laws with monotonically increasing slopes (with slope defined as $\alpha = d \log S_\nu / d \log \nu$; Cruz-Gonzales & Huchra 1984; Ghisellini et al. 1986; Brown et al. 1989). A parabolic curve in the log F_ν–log ν plane follows the overall spectral shape with a reduced number of parameters (Landau et al. 1986), but generally fails to fit the spectrum in specific wavelength bands (and the extrapolated fit is very poor at X-ray energies). Therefore, we prefer to characterize the spectrum by power-law slopes in wavelength ranges as wide as is compatible with a reasonable value of χ^2. Looking at Figure 2, it is natural to choose the following intervals:

(i) α_r from 4.8 to 37 GHz;
(ii) α_{mm} from 90 GHz to 0.8 mm;
(iii) α_{ir} using the *JHK* colors;
(iv) α_{opt} using the *BVRI* colors.

A χ^2 test was used to assess the goodness of fit in each spectral region.

The resulting spectral indices are listed in Table 2, along with the 90% confidence error, the χ^2 value for the fit, and the number of points (n) used to perform the fit. (The number of degrees of freedom is $n - 2$, since we are fitting a two-parameter model to the data.) As shown in Figure 2, the spectrum is slightly rising ($\alpha_r = 0.24$) in the centimeter region, peaks at 37 GHz, steepens significantly above 90 GHz to $\alpha_{mm} = -0.75$ in the millimeter range, and steepens further to $\alpha \sim -2$ at infrared and optical wavelengths.

Since the optical data are characterized by fast variability, we compared spectral indices on the first and last nights of *BVRI* observations (January 2–3 and 5–6). As shown in Table 2, no significant spectral change was detected, although as a result of the large uncertainties ($\Delta\alpha_{opt} = 0.13$) the limits are not very stringent. The IR and optical slopes are very similar, but a combined fit gives $\alpha_{ir-opt} = -1.61$ with a $\chi^2 = 106$, indicating that the spectrum is not well represented by a single power law in the full range. As already suggested in § 3.1, this result is probably a consequence of the nonsimultaneity of the optical and infrared data.

According to the χ^2 values in Table 2, a power law is an adequate description of the spectrum in all spectral regions other than the millimeter. The millimeter/submillimeter spectrum seems to be more complex. An enlargement of this part of the spectrum is shown in Figure 3 together with data obtained on 1991 April 8 (Litchfield et al. 1995) and in 1984 February–April (Brown et al. 1989; Salonen et al. 1987, Teräsranta et al. 1987), when the source was in higher and lower luminosity states, respectively. As already noted by Brown et al. (1989) for a sample of blazars, the millimeter/submillimeter emission generally lies above the extrapolation of the centimeter spectrum, indicating the presence of different emission components. In our spectrum, an emission component with self-absorption frequency at ~37 GHz is clearly present. The IRAM data (at 90 and 230 GHz) indicate a rather steep slope, typical of optically thin synchrotron spectra; however, the JCMT data (at 150, 270, and 370 GHz) indicate an emission shoulder with respect to the extrapolation from lower frequencies. This is due to the JCMT fluxes at 150 and 270 GHz being similar, while the 230 GHz IRAM flux is lower. The apparent dip at 230 GHz may be caused by intercalibration problems between the two different instruments, or the excess emission may be the signature of a further synchrotron component with still higher self-absorption frequency. The latter point is discussed in the next section.

TABLE 2

SPECTRAL INDICES

Index	Spectral Range	α	σ_α(90%)	χ^2	n[a]
α_r	4.8–37 GHz	0.24	0.02	2.5	5
α_{mm}	90–375 GHz	−0.75	0.06	35	5
α_{ir}	*JHK*	−2.16	0.17	4.6	3
α_{opt}	*BVRI*	−2.02	0.07	0.1	4
α_{ir-opt}	*JHKBVRI*	−1.61	0.02	106	7
α_{opt1}	*BVRI* (Jan 2–3)	−1.81	0.13	0.1	4
α_{opt2}	*BVRI* (Jan 5–6)	−2.08	0.13	0.1	4

[a] Number of points used to perform the fit.

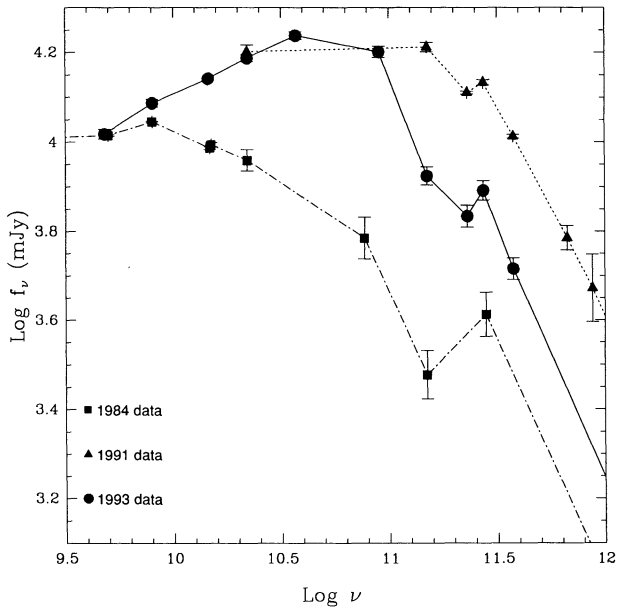

FIG. 3.—Three radio-through-millimeter spectra of 3C 279, taken in 1984, 1991, and during our 1993 campaign. A second peak is clearly visible at millimeter wavelengths in all the spectra. This peak may represent the onset of a new flare, corresponding to the (predicted) emergence of a new VLBI component.

It is important to note that the power per decade (νF_ν) increases from radio to millimeter wavelengths and decreases from infrared to optical wavelengths, meaning a maximum must occur in between, at the frequency for which the spectral index is $\alpha = -1$ (approximately the "break frequency" in the flux density spectrum). The location of such maximum is important for physical models of the source, since it determines the total power and critical frequency range of the synchrotron emission. Extrapolating the millimeter and infrared-plus-optical power-law fits reported in Table 2, the maximum should occur above 10^{13} Hz. A substantial uncertainty in this procedure is introduced by the indication of a steeper slope above 270 GHz (from JCMT data). If the emission above the latter frequency is caused by a single optically thin component with $\alpha \simeq -1$, then the peak frequency in the power per decade could be as high as 10^{14} Hz.

A flatter spectral index in the millimeter range ($\alpha = -0.35$) was derived by Litchfield et al. (1995) for a quiescent state of the source at different epochs. For this reason their determination of the break frequency was lower than the value obtained here (see their Fig. 2).

A reliable determination of the far-infrared spectrum must await the results of the *Infrared Space Observatory* (*ISO*). We stress that the submillimeter to far-infrared spectral region is of crucial importance in determining the link between the optically thin IR radiation and the self-absorbed components observed at low frequencies.

4. DISCUSSION

Present models of blazar emission involve a relativistic jet pointed near the line of sight. Relativistic bulk motion of the emitting plasma is the simplest way to solve paradoxes associated with the excessive brightness temperature and is supported by the apparent superluminal expansion of the parsec-scale radio knots.

In the relativistic jet, particles must be accelerated to high energies and radiate their energy through interactions with both the magnetic field (synchrotron emission) and local soft radiation fields (Compton scattering). The soft radiation field in the jet may be dominated by photons produced within the jet itself or by photons produced in surrounding regions (accretion disk, broad-line clouds, etc.).

Many authors have developed models to account for the observed broadband spectra of blazars. Most of them attribute the radio-to-optical emission to synchrotron radiation, while Compton scattering is invoked for producing the X- through gamma-ray emission (e.g., Marscher 1980; Königl 1981; Reynolds 1982; Ghisellini, Maraschi, & Treves 1985; Maraschi et al. 1992; Bloom & Marscher 1993; Dermer et al. 1992; Sikora et al. 1994; Blandford 1993; Blandford & Levinson 1995). The models differ in the location and structure of the acceleration and emission region(s); some authors concentrate on a single shock front, while others model an inhomogeneous jet where particle acceleration and radiation are assumed to occur continuously along the jet. The latter models may approximate more realistic computations in which energy dissipation in the inner region of the jet results from a series of quasi-stationary shocks (for example, see the hydrodynamic models of Marti et al. 1995).

Furthermore, the flux and spectral variations in blazars can be caused by shock waves propagating along the jet (Marscher & Gear 1985; Hughes, Aller, & Aller 1989; Celotti, Maraschi, & Treves 1991; Valtaoja et al. 1992). The problem is so complex that we are still far from a realistic description of the phenomenon, but the temporal evolution of such flares is qualitatively similar from one model to the next: outbursts occur first at IR-optical frequencies and then propagate to successively longer wavelengths (Marscher & Gear 1985; Valtaoja et al. 1992).

Here we discuss the results on 3C 279 within this general framework. In fact, the millimeter flaring behavior of 3C 279, monitored over several years, is well modeled by evolution of the self-absorption frequency of a synchrotron component, as clearly shown by Litchfield et al. (1995).

In the low state of 1993 January, the synchrotron emission seems to become optically thin above $\sim$90 GHz (see Fig. 2 and Table 2), but at millimeter wavelengths the spectrum appears more complicated than a single, optically thin, power law. The flat spectral shape between 150 and 270 GHz might be caused by an additional self-absorbed synchrotron component, in which case the millimeter-emitting region must have higher electron densities and/or magnetic fields than that responsible for the centimeter emission. Indeed, it is likely that the jet is not as smooth as the inhomogeneous models assume, and not as simple as the single shock model assumes, and that the centimeter and millimeter spectra are dominated by different regions in the jet. The fact that the millimeter excess is present in spectra of very different intensity could indicate that a highly self-absorbed synchrotron component may be present at different intensity levels. Note, however, that no similar millimeter excesses are found in a survey of 24 OVV quasars (including 3C 279) by Gear et al. (1994).

Multiple shocks are evidenced also by the distinct VLBI components, which however refer to regions further out along the jet (Wehrle et al. 1995). The observed millimeter excess could in fact be associated with a newly emerging VLBI component. In this case, the millimeter increase should be followed by a rise in flux at lower radio frequencies, the delay being caused by optical depth effects in the inhomogeneous region, and VLBI maps obtained later in 1993 should show a new knot. In fact we note that the centimeter to millimeter light curves measured by Litchfield et al. (1995) during the whole of 1993 up to mid-1994 show an increasing trend, with a relative peak around 1993 March at the shortest wavelengths.

The power-law spectral slopes between 90 and 150 GHz and between 270 and 370 GHz are similar, $\alpha \sim -1.2$. This suggests that the optically thin synchrotron radiation is produced by similar distributions of relativistic particles, with $s = 2\alpha + 1 \sim 3.4$ (where the electron energy dependence is described by $N_e \propto \gamma_e^{-s}$), in the two different centimeter and millimeter regions. The two VLBI images taken close in time to the campaign seem to confirm this point. Both the 5 GHz and 22 GHz maps show a compact, inhomogeneous radio core and two optically thin blobs with the same radio spectral slope, $\alpha_r \sim -1.2$ (Wehrle et al. 1995). This implies that the acceleration of radiating particles is similar from blob to blob, suggesting that it is not strongly sensitive to local conditions (magnetic fields, pressure, etc.). This is indeed the case for shock acceleration models, in which the slope of the distribution of the accelerated particles reaches a fixed value in the strong shock limit (e.g., Bregman & Boisseau 1989; Fritz & Webb 1990).

The extreme faintness of the source in the optical band at the time of our observations may be related to its steep IR-optical spectrum. Comparing our IR slope (Table 2) with the values measured by Litchfield et al. (1995) in their extensive long-term monitoring, we find that it is the steepest value observed and fits well the correlation between IR flux and spectral index derived by Litchfield et al.

The light curves from our ground-based monitoring of 3C 279 contain important information on the short-timescale evolution of the optically thin IR-optical radiation, which should be related to the basic processes of particle acceleration and radiation in the jet. The observed trends are an increase in flux of $\sim$20% at 37 GHz and $\sim$100% in the R band over the same time interval. If the two flares are related, the different amplitudes could be associated with the spectral hardening expected in the acceleration process at a shock. The fact that the IR-optical spectrum is much steeper than the millimeter one suggests that radiation losses become important at high energies. The faster variability at high frequencies may be caused by the decreasing radiation timescales and/or to smaller emitting regions.

Another important constraint is that at the same time the optical emission was increasing rapidly, no variability

larger than 20% was observed in the X-ray light curve (Maraschi et al. 1994). If the X-rays are the result of inverse-Compton scattering, the lack of correlated variability excludes the possibility that the optical synchrotron photons are the seed photons and/or that the relativistic electrons radiating via synchrotron in the optical band are responsible for scattering other seed photons to X-ray energies.

This is consistent with the spectral constraints: in fact, the synchrotron and inverse Compton spectra produced by the same electrons should have the same slope. In the case of 3C 279, even in the low state, the X-ray spectrum is much flatter than the optical IR one (Maraschi et al. 1994). The only frequency range in which the synchrotron spectrum could match the X-ray slope is between 10^{12}–10^{13} Hz (see Fig. 2). Therefore, the X-rays should derive from electrons radiating at frequencies below the IR-optical bands.

It should be recalled that the flat slope derived in the millimeter range may result from the superposition of different components and that the spectral shape in the range above ~ 400 GHz is presently unknown. Only upper limits are available from the *IRAS* observations. ISO observations will be crucial to clarify this point.

The frequency at which the synchrotron photons have their maximum energy density is the break frequency depicted in Figure 2. If the seed photons for the inverse Compton process are the synchrotron ones, the typical frequency should be between 10^{13}–10^{14} Hz, requiring electrons with Lorentz factors $\gamma \simeq 100$ to produce the observed X-rays. These electrons would radiate via synchrotron in the 10^{10}–10^{11} B Hz range; thus, X-ray variability should be correlated with centimeter-band variability. In fact, correlation studies of 3C 279 on a timescale of years (Grandi et al. 1994) suggest that the X-ray emission is linked to the radio photons rather than to the optical photons.

If the seed photons are external photons of typical frequency $\sim 10^{15}$ Hz, seen in the jet frame at $\sim 10^{16}$ Hz (for $\delta \sim 10$), the scattering electrons needed to produce X-rays must be of very low energy (Lorentz factors $\lesssim 10$). For such low energies, the synchrotron emission would be self-absorbed, therefore unobservable. This does not exclude a correlation of X-ray and radio emission, if the spectrum of the relativistic particles changes in a correlated way over several decades in energy.

The discussion is further complicated by the (likely) possibility that both synchrotron and inverse Compton radiation are produced at various locations in the jet. In this case it is impossible to draw general conclusions without considering specific models, which is beyond the scope of this paper. We think, however, that the link between X-ray photons and the low-frequency region of the synchrotron spectrum (at radio to millimeter wavelengths) is a robust one.

5. SUMMARY AND CONCLUSIONS

We have presented ground-based observations of 3C 279 obtained during the multifrequency campaign of 1992 December–1993 January and have discussed in detail the spectral shape and time variability from radio through optical wavelengths. The main results are as follows:

1. 3C 279 has a typical blazar spectrum, flat and even rising at centimeter wavelengths, then progressively steeper above the turnover frequency which is located between 37 and 90 GHz. In the millimeter part of the spectrum, an additional emission component is suggested which becomes transparent above ~ 270 GHz. In terms of an inhomogeneous or multiple shock model, we interpret the millimeter excess as a region with higher electron density and/or higher magnetic field than that responsible for the longer wavelength radio emission. It may in fact represent a region where a new flare is originating and a new VLBI blob is in formation.
2. The luminosity of 3C 279 varied at radio-millimeter and optical wavelengths during the campaign. The fastest and largest amplitude variability occurred in the R band, where the flux doubled in two weeks. In the same period, an increasing trend with 20% amplitude was observed at 37 GHz.
3. The doubling of flux observed in the optical light curve is not matched by a corresponding increase in X-ray flux. This excludes the possibility that the X-ray photons are produced by scattering of the optical synchrotron photons or by the electrons radiating via synchrotron in the optical band. In agreement with the shape of the observed energy distribution, the X-ray photons should be Compton linked to electrons radiating in the centimeter-millimeter bands. This is a rather general conclusion. Although the superposition of different components may complicate interpretation, direct verification of correlated variability in these bands would be of fundamental importance.

REFERENCES

Aller, H. D., Hughes, P. A., & Aller, M. F. 1991, in Variability of Active Galactic Nuclei, ed. H. R. Miller & P. J. Wiita (Cambridge: Cambridge Univ. Press), 184
Bessel, M. S. 1979, PASP, 91, 589
Blandford, R. D. 1993, in AIP Conf. Proc. 280, Compton Gamma-Ray Observatory, ed. M. Friedlander, N. Gehrels, & D. J. Macomb (New York: AIP), 533
Blandford, R. D., & Levinson, A. 1995, ApJ, 441, 79
Bloom, S. D., & Marscher, A. P. 1993, in AIP Conf. Proc. 280, Compton Gamma-Ray Observatory, ed. M. Friedlander, N. Gehrels, & D. J. Macomb (New York: AIP), 578
Bonnell, J. T., Vestrand, W. T., & Stacy, J. G. 1994, ApJ, 420, 545
Bregman, J. N., & Boisseau, J. R. 1989, ApJ, 347, 118
Brown, L. M. J., et al. 1989, ApJ, 340, 129
Carter, B. S. 1990, MNRAS, 242, 1
Celotti, A., Maraschi, L., & Treves, A. 1991, ApJ, 377, 403
Cotton, W. D., et al. 1979, ApJ, 229, L115
Cruz-Gonzales, I., & Huchra, J. P. 1984, ApJ, 89, 441
Dermer, C. D., Schlickeiser, R., & Mastichiadis, A. 1992, A&A, 256, L27
Duncan, W. D., Robson, E. I., Ade, P. A. R., Griffin, M. J., & Sandell, G. 1990, MNRAS, 243, 126
Fritz, K.-D., & Webb, G. M. 1990, ApJ, 360, 387
Gear, W. K., et al. 1994, MNRAS, 267, 167
Ghisellini, G., Maraschi, L., & Treves, A. 1985, A&A, 146, 204
Ghisellini, G., et al. 1986, ApJ, 310, 317
Grandi, P., et al. 1994, Adv. Space Res., 15 (5), 23
Königl, A. 1981, ApJ, 243, 700
Kniffen, D. A., et al. 1993, ApJ, 411, 133
Hartman, R. C., et al. 1992, ApJ, 385, L1
———. 1995, BAAS, 25, 1450
Hughes, P. A., Aller, H. D., & Aller, M. F. 1989, ApJ, 341, 54
———. 1991, ApJ, 374, 57
Landau, R., et al. 1986, ApJ, 308, 78
Litchfield, S. J., Stevens, J. A., Robson, E. I., & Gear, W. K. 1995, MNRAS, in press
Maraschi, L., et al. 1994, ApJ, 435, L91
Maraschi, L., Ghisellini, G., & Celotti, A. 1992, ApJ, L5
Marscher, A. P. 1980, ApJ, 235, 386
Marscher, A. P., & Gear, W. K. 1985, ApJ, 298, 114
Marti, J. A., Gomez, J. L., Marscher, A. P., Ibanez, J. M., & Marcaide, J. M. 1995, in 17th Texas Symp. on Relativistic Astrophysics, in press
Makino, F., et al. 1989, ApJ, 347, L9

Makino, F. 1992, in Frontiers of Neutrino Astrophysics, ed. Y. Suzuki & K. Nakamura (Tokyo: Universal Academy Press), 425
Mead, A. R. G., Ballard, K. R., Brand, P. W. J. L., Hough, J. H., Brindle, C., & Bailey, J. A. 1990, A&AS, 83, 183
Pica, A. J., Pollock, J. T., Smith, A. G., Edwards, P. L., & Scott, R. J. 1980, AJ, 85, 1442
Reynolds, S. P. 1982, ApJ, 256, 13
Sadun, A. C., Fajardo, S., & Carini, M. T. 1992, in Variability of Active Galactic Nuclei, ed. H. R. Miller & P. J. Wiita (Cambridge: Cambridge Univ. Press), 131
Salonen, E., et al. 1987, A&AS, 70, 409
Sandell, G. 1994, MNRAS, 271, 75
Shrader, C. R., et al. 1994, AJ, 107, 904
Sikora, M., Begelman, M. C., & Rees, M. 1994, ApJ, 421, 153
Steppe, H., Liechti, S., Mauersberger, R., Kömpe, C., Brunswig, W., & Ruiz-Moreno, M. 1992, A&AS, 96, 441
Steppe, H., Salter, C. J., Chini, R., Kreysa, E., Brunswig, W., & Lobato Perez, J. 1988, A&AS, 75, 317
Stevens, J. A., Litchfield, S. J., Robson, E. I., Hughes, D. H., Gear, W. K., Teräsranta, H., Valtaoja, E., & Tornikoski, M. 1994, ApJ, 437, 91
Stevens, J. A., & Robson, E. I. 1994, MNRAS, 270, L75
Takalo, L. O., Sillanpaa, A., Nilsson, K., Kidger, M., de Diego, J. A., & Piirola, V. 1992, A&AS, 94, 37
Teräsranta, H., et al. 1987, A&AS, 71, 125
———. 1992, A&AS, 94, 121
Tornikoski, M., et al. 1995, A&AS, submitted
Unwin, S. C., Biretta, J. A., Hodges, M. W., & Zenzus, J. A. 1989, ApJ, 340, 117
Urry, C. M., et al. 1995, in preparation
Valtaoja, E., Teräsranta, H., Urpo, S., Nesterov, N. S., Lainela, M., & Valtonen, M. 1992, A&AS, 254, 71
von Montigny, C., et al. 1995, ApJ, 440, 525
Webb, J. R., Carini, M. T., Clemens, S., Fajardo, S., Gombola, P. P., Leacock, R. J., Sadun, A. C., & Smith, A. G. 1990, AJ, 100, 1452
Wehrle, A. E., et al. 1995, in preparation
Whitney, A. R., et al. 1971, Science, 173, 225
Zbyszewska, M. 1993, in AIP Conf. Proc. 280, Compton Gamma-Ray Observatory, ed. M. Friedlander, N. Gehrels, & D. Macomb (New York: AIP), 608